Confinement and Transport in EC heated RI-mode discharges in TEXTOR-94

G.M.D. Hogeweij[1], P. Dumortier[2], J.C. van Gorkom[1], R.J.E. Jaspers[1], D. Kalupin[3], R.H. Koslowski[3], A. Messiaen[2], R.W. Polman[1], F.C. Schüller[1], B. Unterberg[3], M. Vervier[2], G.van Wassenhove[2], E.Westerhof[1]

[1] *FOM Instituut voor Plasmafysica 'Rijnhuizen', Associatie EURATOM-FOM, Trilateral Euregio Cluster, P.O.Box 1207, 3430 BE Nieuwegein, The Netherlands*

[2] *Laboratoire de Physique des Plasmas-Laboratorium voor Plasmafysica, Association EURATOM-Belgian State, ERM/KMS, Brussels, Belgium*

[3] *Institut für Plasmaphysik, FZ Jülich GmbH, EURATOM Ass., Jülich, Germany*

1. Introduction

The effect of Electron Cyclotron Heating (ECH) on the performance of Radiatively Improved (RI) mode discharges in TEXTOR-94 [1, 2] is reported. For the experiments one gyrotron was used, pulse length 200 ms, delivering into the plasma effectively 250 kW, 110 GHz power in 2nd harmonic X-mode.

2. Global Effects of ECH

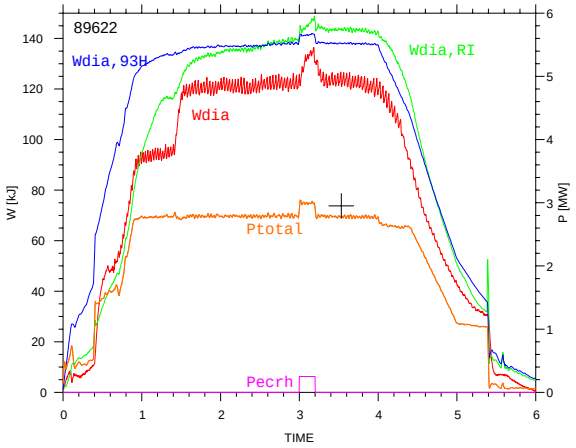

Figure 1: *W_{dia}, W_{RI} and W_{93H} (red, green, blue, in kJ, left axis), total input power and ECH power (P_{tot}, orange, P_{ECH}, pink, in MW, right axis) of discharge 89622. Plasma parameters: $I_p = 400$ kA, $B_t = 2.08$ T, $\langle n_e \rangle = 5.5 \cdot 10^{19}\mathrm{m}^{-3}$.*

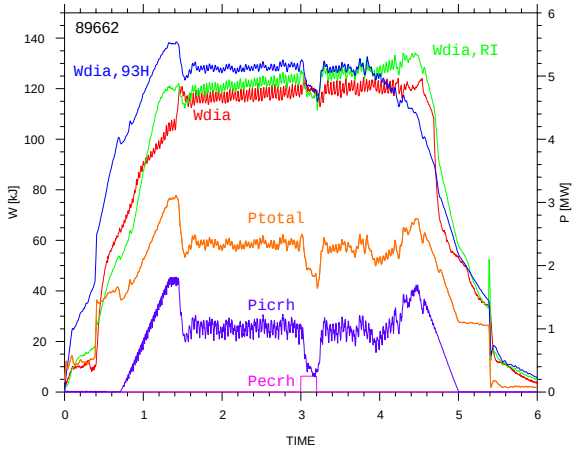

Figure 2: *Discharge 89662, where P_{ICRH} was under feedback of W_{dia} (feedback value 120 kJ). Shown are the signals in the same colours as in Fig.1, plus the ICRH power. Plasma parameters as in Fig.1.*

ECH with central resonance ($B_T \simeq 2.08$ T) was applied to RI-mode discharges in TEXTOR at several values of plasma current ($300 \leq I_p[\mathrm{kA}] \leq 450$) and line integrated density ($3 \leq \langle n_e \rangle [10^{19}\mathrm{m}^{-3}] \leq 6.5$). We compare the performance with and without ECH using the RI-mode scaling:

$$\tau_{RI} = 0.18 \cdot \langle n_e \rangle \cdot P_{tot}^{-2/3} \qquad (1)$$

with τ_{RI}, $\langle n_e \rangle$ and P_{tot} in sec, $10^{20}\mathrm{m}^{-3}$ and MW, respectively [1]. In the plots also the ITER-93H scaling, τ_{93H}, is shown. The energy content expected on basis of these scalings will be denoted by W_{RI} and W_{93H}. As $P_{ECH}/P_{tot} \simeq 0.25/2.7[\mathrm{MW}] \simeq 9$ %, (in fact even less, since P_Ω drops during ECH), Eq.1 would predict a relative increase of stored energy (δW_{dia}) of typically 3 %. However, in many cases $\delta W_{dia}/W_{dia} \simeq 9\%$ is observed, i.e. ECH is remarkably effective. See Fig.1 for an example.

In a few discharges P_{ICRH} was under feedback of a preset value of W_{dia}. In this way the effectiveness of ECH could be compared directly with that of ICRH. In many cases 250 kW of ECH was as effective as 750 kW of ICRH, thus confirming the improved confinement during ECH; see Fig.2 for an example. It should be noted, however, that the value of B_t was slightly lower than the optimum value for central ICRH resonance.

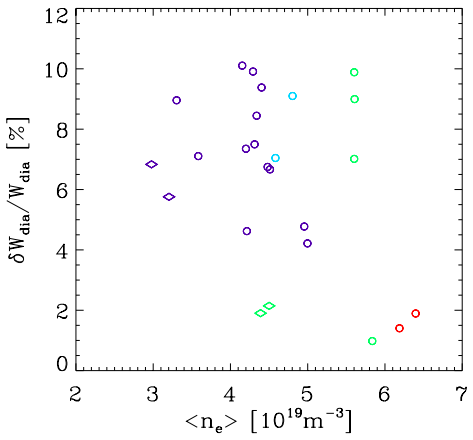

Figure 3: *Plot of $\delta W_{dia}/W_{dia}$ vs. $\langle n_e \rangle$ for RI-mode discharges with central ECH. Plasma parameters: I_p = 300, 350, 400 and 450 kA (dark blue, light blue, green, red, respectively) and B_t = 2.08 T. The diamonds represent L-mode discharges with ECH.*

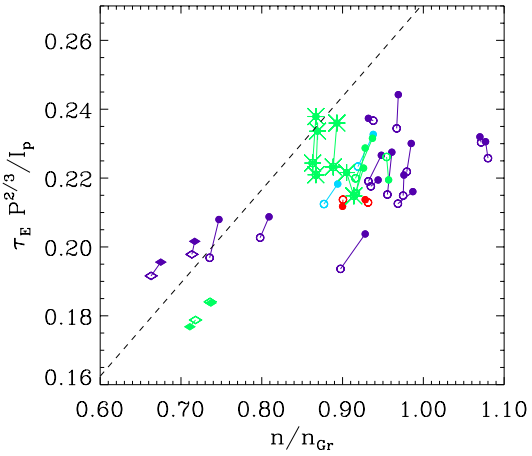

Figure 4: *Plot of $\tau_E P_{tot}^{2/3}/I_p$ vs. normalized density for the discharges of Fig.3. Closed (open) symbols: phase with (without) ECH. Colors and symbols as in Fig.3. The 4 discharges with P_{ICRH} under feedback are marked with a large asterisk. The standard RI-mode scaling, Eq.1, is given by a dashed line.*

In Fig.3 $\delta W_{dia}/W_{dia}$ is plotted for a number of discharges. The effectiveness of ECH is seen to hold up to $\langle n_e \rangle \simeq 5.5 \cdot 10^{19}\mathrm{m}^{-3}$, corresponding to $n_e(0) \sim 8.5 \cdot 10^{19}\mathrm{m}^{-3}$, which is clearly above the 110 GHz cut-off density of $\simeq 7.5 \cdot 10^{19}\mathrm{m}^{-3}$. In fact, central ECE channels are in cutoff when $\langle n_e \rangle \geq 4.3 \cdot 10^{19}\mathrm{m}^{-3}$. In comparable L-mode discharges (also shown in this plot), the increase of W_{dia} was close to the expected 3%.

The performance of the EC heated RI-mode discharges can be appreciated in the diagram of $\tau_E P_{tot}^{2/3}/I_p$ vs. n_e/n_{Gr}, where n_{Gr} is the Greenwald density. The RI-mode scaling shows up as a straight line in this diagram. In Fig.4 a number of discharges are shown in this way. Each discharge is represented by two points: one for the average performance during ECH, and one for the RI-phase without ECH; the latter is the average value of the phase just before switch-on of ECH and after switch-off of ECH (in order to get rid of possible slow trends in the time traces, e.g. a slow density increase during the discharge). There is a small but striking improvement of performance during ECH.

3. Comparison of L-mode with RI-mode

To study the transition from L-mode to RI-mode, a neon scan was performed: in five discharges the level of neon puffing was increased from 0 (L-mode) to the highest possible level (i.e. staying just below the density limit). Fig.5 shows time traces of these five discharges. In Fig.6 T_e and n_e profiles from Thomson scattering (TS) from the same five discharges are plotted (the profiles are taken just before the end of the ECH pulse). With increasing neon content the n_e profile is seen to peak, whereas the T_e profile hardly changes. This peaking of n_e is reflected in the increasing W_{dia} with increasing neon puff.

The change in sawtooth behaviour in this scan is striking. This can already be seen on some time traces in Fig.5, but is much clearer documented by the 3rd harmonic ECE

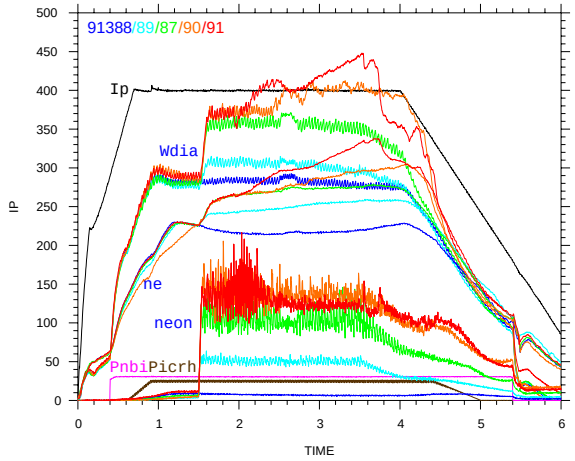

Figure 5: *Time traces of five TEXTOR discharges with increasing neon puff, and otherwise similar parameters (colors from blue, via cyan, green and orange, to red). Shown are I_p, W_{dia}, n_e, neon puff, P_{ICRH}, P_{NBI} and P_{ECRH}. The y-axis ranges are 200 kJ, $5{\cdot}10^{19}\mathrm{m}^{-3}$ and 20 MW for W_{dia}, n_e and the NBI and ICRH powers, respectively; the ECH power and neon puff are in arbitrary units.*

signals in Fig.8 (the 2nd harmonic ECE, normally used for T_e measurement, is in cut-off). The sawtooth behaviour changes from normal to humpback-like at the highest neon puff level; interestingly, ECH appears to trigger a similar change in cases where the neon puff is rather strong. It should be noted that this ECH related sawtooth change occurs in cases where $n_e(0)$ is above the ECH cut-off density, so it might be related to off-axis heating due to refraction of the ECH beam.

The neon scan was performed at high I_p and n_e. However, similar behaviour can be seen at more modest plasma parameters: Fig.7 compares TS T_e and n_e profiles from from an L-mode discharge with ECH with two RI-mode discharges, one with and one without ECH, all at $I_p = 300$ kA. The RI-mode cases have much more peaked n_e compared to L-mode; application of central ECH in RI-mode causes a strong peaking of T_e.

4. Local Transport

In order to study local transport, scans of the ECH power deposition radius (ρ_{dep}) were made, both by varying B_{tor} and by tilting the poloidal mirror of the ECH launching system, at different plasma conditions. As an example, Fig.9 shows results of a poloidal mirror scan at high I_p and $\langle n_e \rangle$ (400 kA, $5.5 \cdot 10^{19}\mathrm{m}^{-3}$). The effect of ECH heating shows a step like change from strong to weak increase of W_{dia} near $\rho = 0.3$. This indicates that a region of low (electron) heat transport exists around $\rho = 0.3$, which corresponds with the location of $q = 1$. In a scan at lower I_p, $\langle n_e \rangle$ (300 kA,$4.2 \cdot 10^{19}\mathrm{m}^{-3}$) this sharp change from strong to weak increase of W_{dia} was found to be near $\rho = 0.25$, which is near or just outside $q = 1$.

5. Discussion and Conclusions

In spite of the modest level and duration of the current ECH power very intersting results have been obtained, in terms of confinement improvement and change of sawtooth activity. It is expected that these results can be extended when a new gyrotron (140 GHz, 1 MW, 3-10 s) is available in 2002.

An ongoing effort in transport analysis and modelling is being performed, focusing on the understanding of profile peaking and sawtooth reduction.

Acknowledgements. This work was performed under the Euratom-FOM association agreement, with financial support from NWO and Euratom.

References

[1] Weynants, R.R., et al, *Nucl. Fusion* **39** (1999) 1637
[2] Ongena, J., et al, *Plasma Phys. Contr. Fusion* **41** (1999) A379
[3] Kalupin, D., et al, *this conference*

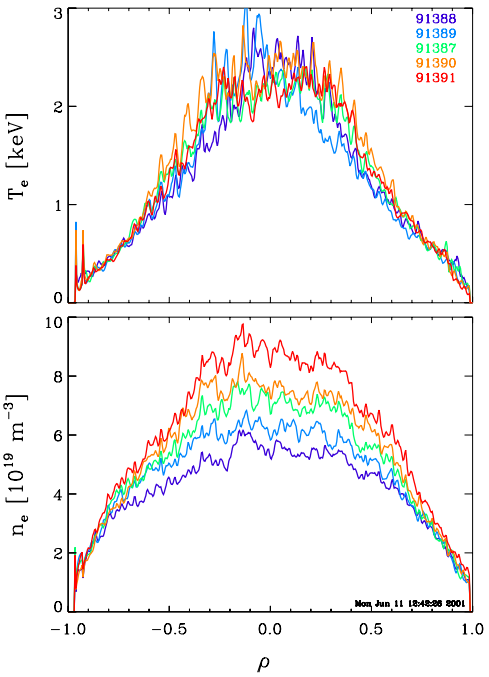

Figure 6: *Profiles of T_e and n_e from TS, for the same five discharges and in the same color coding as in Fig.5.*

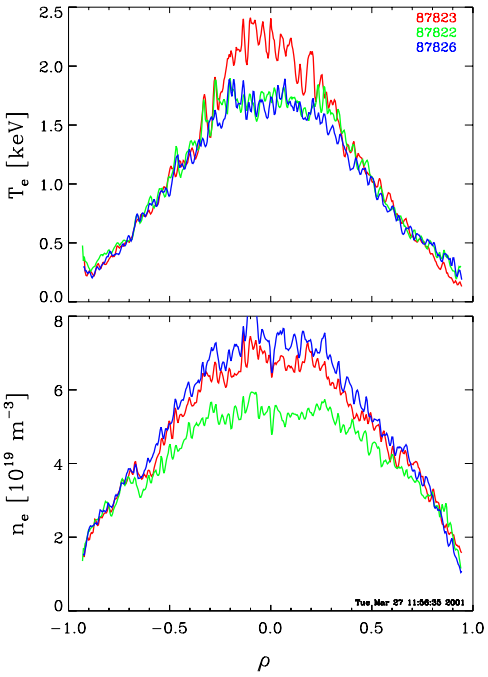

Figure 7: *TS T_e and n_e, of three discharges: L-mode with ECH (blue), RI-mode without ECH (green), RI-mode with ECH (red).*

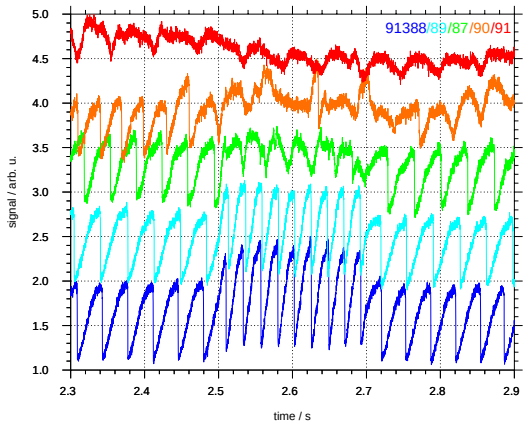

Figure 8: *Third harmonic ECE time traces, coming from the centre of the plasma, for the 5 shots of Fig.5, with the same colors.*

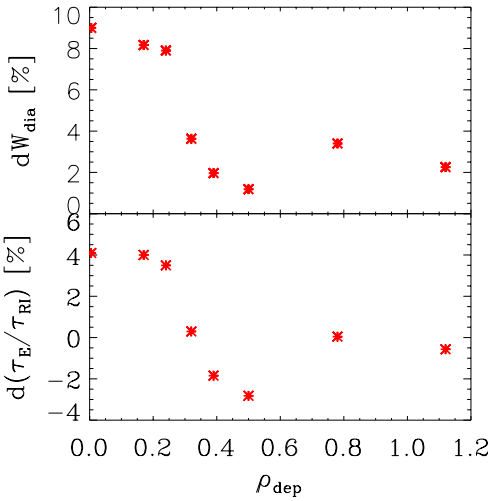

Figure 9: *$\delta W_{dia}/W_{dia}$ and $\delta(\tau_E/\tau_{RI})$ vs. ρ_{dep} for 8 discharges with similar parameters ($I_p = 400$ kA, $B_t = 2.08$ T, $\langle n_e \rangle \simeq 5.5 \cdot 10^{19}\mathrm{m}^{-3}$) where ρ_{dep} was varied by tilting the poloidal ECH mirror. Refraction of the ECH beam was taken into account.*